

EBG Placement Optimization in a Via-Fed Stacked Patch Antenna for Full-Duplex Wireless

Adewale K. Oladeinde, Samuel Shippey, Ehsan Aryafar, and Branimir Pejcinovic
Portland State University, Portland, OR, USA

Abstract—Full-Duplex (FD) wireless communication has the potential to double the capacity of a wireless link. The key challenge to FD is self-interference (SI): a node’s transmitting signal generates significant interference to its own receiver. Several prior works have shown the potential to reduce SI and build FD radios but they are limited to Sub-6 GHz systems. In this paper, we focus on the emerging mmWave systems and the potential reduction in SI through antenna design. The increased bandwidth requirements of mmWave systems necessitate the use of higher bandwidth antenna designs such as stacked patch antennas for transmission (Tx) and reception (Rx). Specifically, we investigate the optimal placement of a mushroom electromagnetic band gap (EBG) structure for maximum Tx and Rx isolation (coupling reduction) in a 4-layer substrate stacked patch antenna design targeted for small mobile devices. Through extensive simulations we show that top&inner layer EBG (“stacked”) provides more than 80 dB of isolation at 28 GHz frequency, which is 20 dB more isolation than either top or inner layer EBG. We also show that the frequency bandwidth and gain of the stacked patch antenna are not negatively impacted due to the EBG integration.

Index Terms—Full-duplex wireless, MmWave bands, Electromagnetic band gap, Stacked patch antennas

I. INTRODUCTION

The demand for wireless capacity is exploding due to emergent applications, ranging from augmented and virtual reality (AR/VR) to massive cellular access. The spectrum crunch in the legacy sub-6 GHz radio bands has led to the use of higher frequencies (mmWave bands) due to the large amounts of spectrum available in these bands.

On a parallel front, full-duplex (FD) wireless has recently emerged as a new technology that allows a wireless device to transmit and receive at the same time and on the same frequency. With FD, the transmitting antenna causes a significant amount of self-interference (SI) on the receiving antenna. Given the co-location of the interfering source compared to the farther desired transmission source, this would completely draw the weaker intended signal in interference, rendering its decoding impossible. Thus, the key challenge in enabling FD so far has been to reduce/eliminate SI.

Over the past decade, several works have proposed a variety of SI cancellation techniques to enable FD but they are primarily limited to sub-6 GHz systems (for a survey, refer to [1]). For example, to enable FD at a small handheld device with 19 dBm transmission power and -95 dBm of noise floor, 114 dB of SI needs to be cancelled. Existing designs initially use passive cancellation techniques (e.g., antenna design) and then augment that with active cancellation techniques, which

use SI channel information to remove the remaining SI in the analog and/or digital baseband domains.

More recently, researchers have proposed FD radio designs for mmWave systems. For example, in [2] authors develop mmWave circulators that connect to the same transmit (Tx) and receive (Rx) antennas and reduce SI. On the other hand, using separate Tx and Rx antennas can provide much more reduction in SI due to over-the-air path loss, which can further simplify the design of active SI cancellation techniques. This can lead to compact FD designs that can fit in small mobile devices. In [3], we proposed the design of a new electromagnetic band gap (EBG) structure, coined “VicCross EBG” integrated in a two layer substrate design and showed that the design can help with passive SI cancellation. In this paper, we focus on the EBG placement problem over a 4-layer stacked patch antenna and study how EBG placement can help with SI reduction and its impact on other antenna performance metrics, such as gain and frequency bandwidth. Stacked patch antennas support higher bandwidths and are therefore quite suitable for mmWave systems. Specifically, we focus on conventional mushroom EBGs [4], and do a comprehensive study of EBG placement optimization over a stacked patch antenna. Our contributions are as follows:

- **Design:** We design a unit element stacked patch antenna structure for maximum frequency bandwidth and gain using a 4-layer substrate stack-up design with Rogers RO3003 (3,0.001) material. We consider separate Tx and Rx antenna element structures on the same substrate, place a mushroom EBG between the two for maximum SI reduction, and optimize the placement of three different EBG models referred to as “top layer EBG”, “inner layer EBG”, and “top&inner (stacked) layers EBG”.
- **Evaluation:** Through a combination of theoretical modeling and extensive simulations using High Frequency Structure Simulator (HFSS [5]), we evaluated the sizes and placement of the different EBG models to attain maximum isolation between the Tx and Rx antenna element structures. We show that the multi-layer top&inner layer (stacked) EBG model provides more than 80 dB of isolation (SI reduction), which is approximately 20 dB more than the other EBG model structure placements and 40 dB more than when no EBG is employed. We also show that the integrated EBG models have negligible impact on other antenna performance metrics such as gain and frequency bandwidth.

The rest of this paper is organized as follows. We discuss

our stacked patch antenna model in Section II. We introduce the three different EBG integration models with the stacked patch antenna structures in Section III. We present the results of our extensive simulations in Section IV. Finally, we conclude the paper in Section V.

II. STACKED PATCH ANTENNA MODELS

We consider a stacked patch antenna structure in this paper. Stacked patch antenna structures have received considerable attention due to their wide bandwidth applications¹. This makes stacked patch antennas particularly useful for mmWave systems and radios.

The stacked patch antenna is composed of top and inner layer patches fed through a laser drilled micro-via connected to a 50 Ω transmission line as shown in Fig. 1. The substrate material employed for this design is a Rogers RO3003 material with permittivity and loss tangent of 3.0 and 0.0010, respectively [6]. Substrate thicknesses of 300 μm , 250 μm , and 50 μm were used between the top layer and the first inner layer, first inner layer and second inner layer, and second inner layer and bottom layer, respectively. The thickness of the copper foil is 15 μm . The diameter of the via drill between the first inner layer and the second inner layer is 200 μm with pad diameter of 300 μm . Second inner layer to bottom layer via drill is 100 μm with pad diameter of 200 μm . Grounded co-planar wave-guide transmission line was used to mitigate unwanted mode conversion from propagating on the transmission line to the stacked patch antenna and it connects to a 50 Ω port. A grounded co-planar via pitch of 250 μm is maintained around the transmission line.

Initial theoretical length and width for each patch was calculated and determined using Eqs. (1)-(3) [7] below:

$$W = \frac{v_0}{2f_r} \sqrt{\frac{2}{\epsilon_r}} \quad (1)$$

$$L = \frac{1}{2f_r \sqrt{\epsilon_{reff}} \sqrt{\mu_0 \epsilon_0}} - 2\Delta L \quad (2)$$

$$\Delta L = 0.412 \times \frac{(\epsilon_{reff} + 0.3) \left(\frac{W}{h} + 0.264\right)}{(\epsilon_{reff} - 0.258) \left(\frac{W}{h} + 0.8\right)} \quad (3)$$

here, W , L , and ΔL denote the patch width, patch length, and patch length extension, v_0 is the speed of light in free space, ϵ_r , ϵ_0 , ϵ_{reff} , μ_0 , and h are relative permittivity, permittivity of free space, effective permittivity, permeability, and thickness of the substrate material, and f_r denotes the resonant (desired) frequency of 28 GHz². We further optimized the length and width for the patch antennas using Ansys High-Frequency Structure Simulator (HFSS) to arrive at the required frequency bandwidth of interest.

¹Both stacked and micro-strip patch antennas are easy to manufacture and have a low profile. However, stacked patch antennas support much higher bandwidths, and therefore are mostly used for mmWave systems.

²This frequency band is primarily owned by Verizon in the US and is used in their 5G mmWave deployment. We have recently acquired an FCC experimental license as well as radio hardware to transmit in these bands. We plan to compare the results of our experiments against simulations as part of our future work.

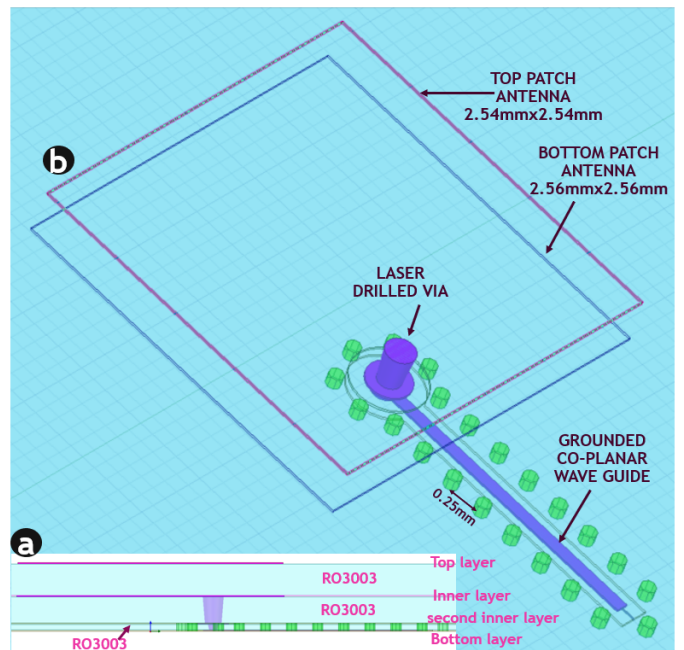


Fig. 1. A single structure micro-via-fed stacked patch antenna. (a): side view showing top, first inner, second inner, and bottom layers. laser drilled micro-via connecting to inner patch. (b): stacked patch showing patch dimensions with co-planar wave-guide transmission line connected to Lump port. The small green dodecagons (12-sided polygons) represent the laser drilled vias.

Fig. 2 shows two stacked patch antennas in the same substrate environment and placed apart at 16 mm pitch³. One stack patch antenna structure represents the Tx antenna, while the other represents the Rx antenna. We use same stacked patch antennas element for transmission and reception and this separation itself contributes up to 40 dB towards SI cancellation as we will show later through simulations in Section IV.

III. STACKED PATCH ANTENNA MODELS WITH INTEGRATED EBGs

Electromagnetic band gap (EBG) structures are periodic structures that introduce frequency band gaps in form of frequency stopband in order to suppress propagation of certain frequencies. EBG structures have many applications, including antenna design and electromagnetic noise suppression [8], [9], [10], among others. More recently, a mushroom EBG [11] has been used to reduce SI and enable FD at the 3.2 GHz frequency band.

In this section, we consider three different mushroom EBG placements in the stacked patch antenna substrate environment resulting in three stacked patch model structures integrated with EBG. EBG structures were integrated between the Tx and Rx antenna elements for further isolation between the two antennas and reduced SI. We refer to these three integrated EBG models as “top layer EBG”, “inner layer EBG”, and “top&inner (stacked) layer EBG”.

³16mm separation was chosen to ensure both Tx and Rx antenna elements are outside their reactive near field and radiating near field distance.

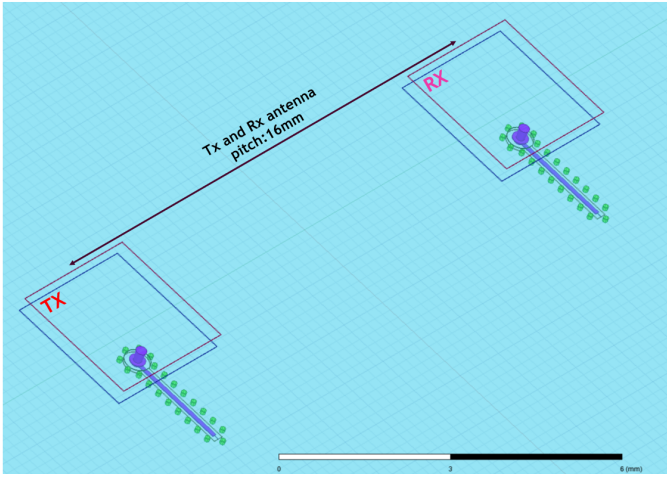


Fig. 2. We use different Tx and Rx stacked patch antennas for transmission and reception, respectively. The antenna separation itself, contributes to substantial reduction in SI.

For each integrated EBG model, we start by an initial analysis to derive the EBG and antenna design parameters. These parameters, which are derived from theoretical calculations, are then optimized through simulations for maximum Tx and Rx isolation (i.e., SI reduction). The final design parameters (patch sizes, EBG pitch, and EBG distance to antennas) are shown in Fig. 3. We describe this process in details next.

A. EBG Configuration

EBG, being a 2D periodic structure, can be classified as mushroom or uni-planar based on the unit cell geometry. Both EBG structures are easy to manufacture and have a simple design. We employed a mushroom EBG in our design.

Equations (4), (5), and (6) were employed to come up with the initial EBG patch and shorting pin inductance and capacitance values in order to obtain the EBG patch size and to suppress propagating surface waves at the desired 28GHz frequency of operation.

The analysis derived from theoretical models [7] serves as a starting point, which is further optimized through HFSS simulations.

$$C = \frac{W\epsilon_0(1 + \epsilon_{reff})}{\pi} \cosh^{-1}\left(\frac{W + g}{g}\right) \quad (4)$$

$$L = 2 \times 10^{-7} \times h \times \left[\ln\left(\frac{2h}{r}\right) + 0.5\left(\frac{2r}{h}\right) - 0.75 \right] \quad (5)$$

$$f = \frac{1}{2\pi\sqrt{LC}} \quad (6)$$

here W is the EBG width, g is the gap between two EBG elements, ϵ_0 and ϵ_{reff} are free space and relative permittivity of substrate material, h is the substrate material thickness, r is the radius of EBG shorting via, L , C and f are the inductance, capacitance, and resonant frequency of the EBG design.

The table in Fig. 3 shows the final EBG parameters (after HFSS simulations and optimization) for each of the three (top, inner, and top& inner) stacked patch antenna models.

	Patch Size (mm)	EBG pitch (mm)	EBG to Antenna edge (mm)	Via Drill diameter (μm)	Via drill Height (mm)
Top Layer EBG	0.7 x 0.7	1.9	0.67	100	0.58
Inner Layer EBG	0.7 x 0.7	1.82	0.91	100	0.27
Top&Inner (Stacked) EBG	0.6 x 0.6	1.9	0.72	100	0.58

Fig. 3. Optimized EBG patch sizes and dimensions for each of the three stacked patch antenna models.

We next discuss the detailed configuration of each of the three stacked patch antenna models.

B. Top Layer EBG Model Structure

Authors in [9] have shown that a higher band gap and isolation effect is achieved when the number of EBG columns is increased. Due to this observation, in our design we employed seven columns of EBG between Tx and Rx antenna structures. Top layer EBG patch (as shown in Fig. 4) is located on the top side of the substrate with its shorting via connected to the second inner ground or reference plane. The size of the EBG patch is 0.7 mm x 0.7 mm with 100 μm diameter and 0.58 mm height shorting via. EBG pitch and spacing to the top stacked patch edge are 1.9 mm and 0.67 mm, respectively.

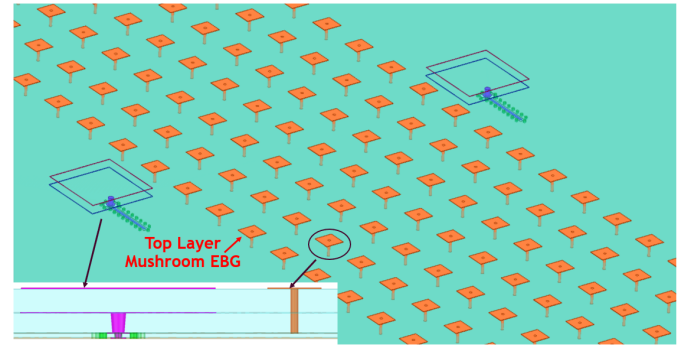


Fig. 4. Top layer EBG model showing the EBG patch on the top substrate layer with its shorting via connected to the second inner layer ground plane. The side view is shown on the bottom left side of the figure.

C. Inner Layer EBG Model Structure

Inner layer EBG patch (as shown in Fig. 5) is located on the inner layer of the substrate design with its shorting via connected to the second inner ground layer. After initial analysis and follow up simulation, inner layer EBG patch was determined to be 0.7 mm x 0.7 mm with 100 μm diameter and 0.27 mm height shorting via. EBG pitch and spacing to inner patch edge are 1.82 mm and 0.91 mm, respectively.

D. Top&Inner Layer EBG Model Structure

In the top&inner layer (stacked) structure, the EBG is located both on the top and inner layers of the substrate forming a stacked EBG with its shorting via connecting both

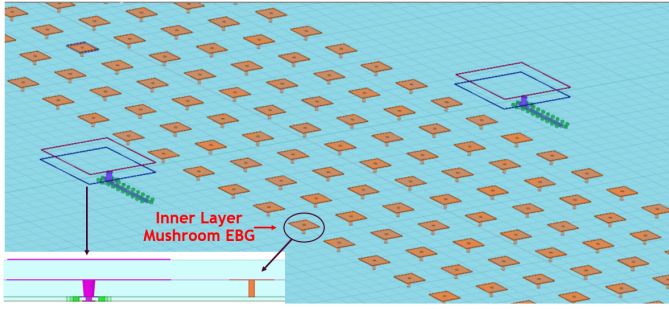


Fig. 5. Stacked Patch antenna integrated with inner layer EBG. The side view is shown on the bottom left side of the figure, which shows the EBG placement at the inner layer.

top and inner EBG patches to the second inner ground. This structure is shown in Fig. 6. The top and inner layer EBG patch sizes were determined to be 0.6 mm x 0.6 mm with 100 μ m diameter and 0.58 mm height shorting via. EBG pitch and spacing to inner patch edge are 1.9 mm and 0.72 mm, respectively.

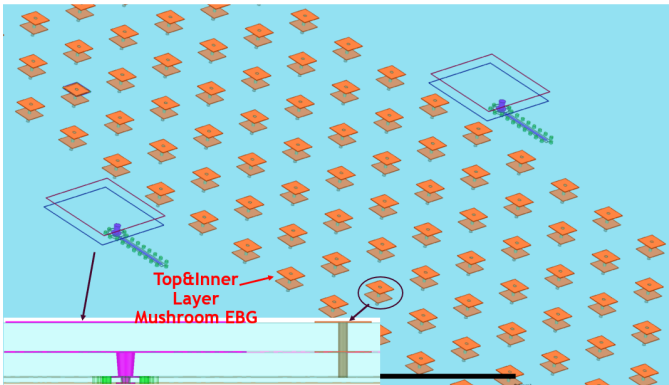


Fig. 6. Stacked patch antenna integrated with Top&Inner layer EBG. The side view is shown on the bottom left side of the figure and depicts this EBG placement.

IV. PERFORMANCE EVALUATION

We compared the performance of our designs using Ansys High-Frequency Structure Simulator tool (Ansys HFSS). As a baseline for comparison, we considered the antenna design with separate Tx and Rx stacked patch antennas without integrated EBG (i.e., Fig. 2). We first discuss the impact of EBG placement (for each of the three models) on two critical antenna performance metrics: frequency bandwidth and gain. Next, we discuss the impact of EBG placement on Tx-Rx isolation (i.e., SI reduction).

Antenna Frequency Bandwidth. Fig. 7 shows the return loss (S-parameter) plot as a function of frequency, which also determines the frequency bandwidth of the stacked patch antenna. In antenna design, a return loss of -10 dB or lower is typically desirable. We observe that all four stacked patch antenna models (three with integrated EBG and one with no EBG) have similar impedance bandwidth of 1.8 GHz at -10 dB

with resonant frequencies at 28.4 GHz and 31.4 GHz. The dual resonant frequencies are the result of the top and inner patches resonating at higher and lower frequencies, respectively. A 2-3 dB degradation at resonant frequencies is observed in antenna models with integrated EBG.

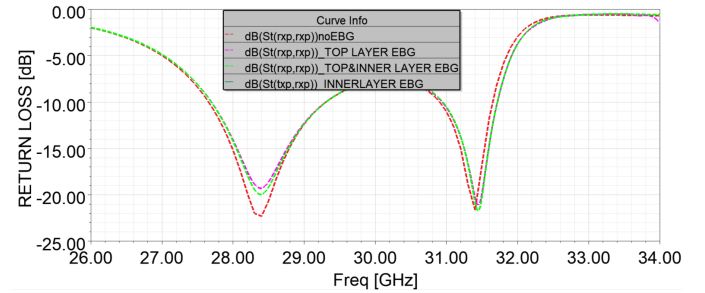


Fig. 7. S-parameter plot showing return loss, which depicts frequency bandwidth of 1.8 GHz at -10 dB with resonant frequencies at 28.4 and 31.4 GHz. All four models achieve a similar frequency bandwidth.

Antenna Gain. Fig. 8 and Fig. 9 depict the E and H plane antenna gains across all four antenna models (three with integrated EBG and one with no EBG), respectively. All four models have a very similar E-plane gain.

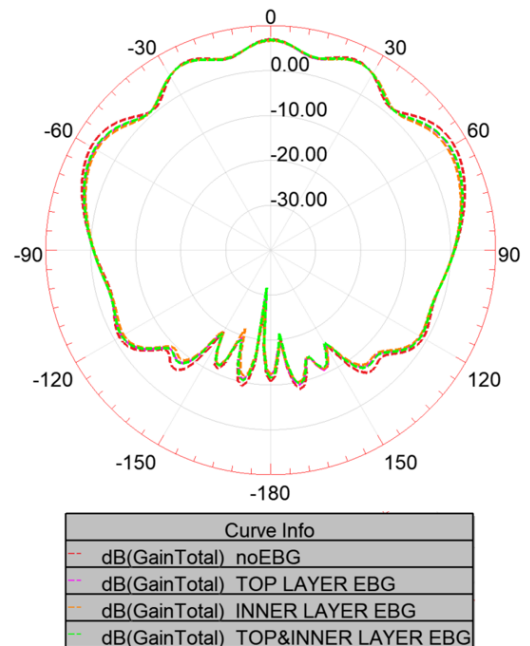


Fig. 8. Stacked patch antenna E-Plane gain plots. All models have almost similar gain and radiation pattern.

An increase of 5 dB in backside lobe level is observed in H plane (Fig. 9) for stacked patch models with integrated EBG. We attribute this to multiple reflection of surface wave on the second inner layer coupled to the bottom layer plane and its interaction (destructive interference) with radiated field.

After careful examination, we concluded that the backside lobe radiation was minimized due to the same substrate material used across all layers in the design. The same substrate

material resulted in no refractive index (n) change seen by the surface wave as it propagates from the inner layer to the bottom layer, hence the minimal reflection resulting to reduced backside lobe. Here $n \propto \sqrt{\mu(r)\epsilon(r)}$ with $\mu(r)$ and $\epsilon(r)$ representing the relative permeability and permittivity of materials. In our designs, we mitigated conditions for multiple surface wave reflections that could impact and cause destructive interference with the propagating electric field from antenna structure through use of the same material substrate and well optimized EBG models integrated within Tx and Rx stacked patch antenna environment. The increased backside lobe radiation is not troubling because it is less than 5 dB which is not enough to cause major radiation interference from one antenna structure (Tx) to another antenna structure (Rx).

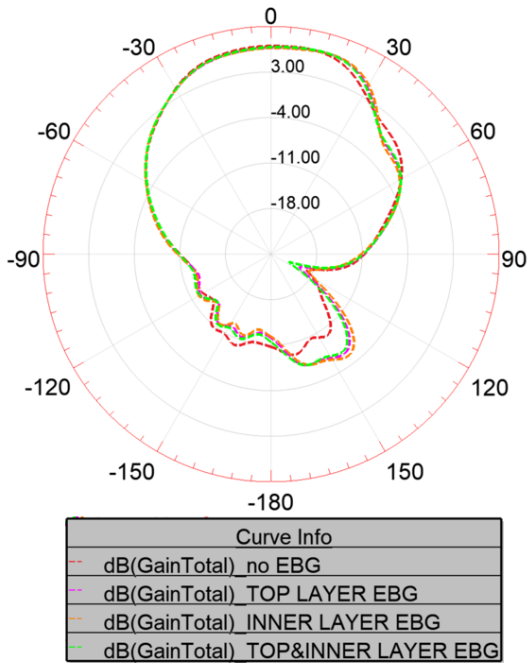


Fig. 9. Stacked Patch antenna integrated with EBG models H-Plane Gain Plots. All models have similar Gain pattern as stacked patch model with noEBG but with increased back lobe radiation due to surface wave reflection on inner layer of the model structure.

Overall, We designed our stacked patch antenna structure to realise maximum gain of 7.2dB as shown in Fig. 10

Tx-Rx Isolation (SI Reduction). Fig. 11 depicts the reduction in Tx and Rx coupling (i.e., the reduction in SI). Top&Inner (stacked) layer EBG provides the highest isolation of 88 dB at 28 GHz. Further, all three EBG integrated antenna models provide a minimum of 60 dB isolation with 160 MHz of bandwidth. There is a minimum of 16 dB additional isolation at 28 GHz frequency compared to the no EBG model. Further, the stacked patch antenna integrated with stacked EBG model provides additional 40 dB of isolation at 28 GHz compared to the no EBG model.

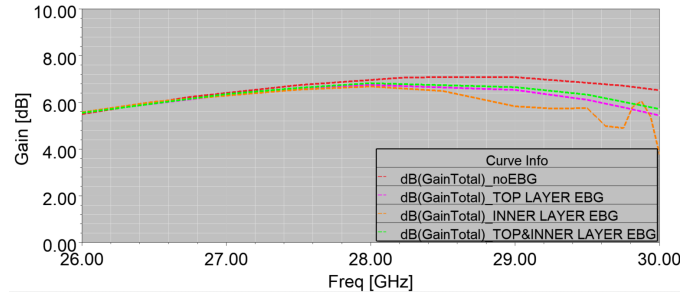


Fig. 10. Maximum Gain plot of all stacked patch antenna integrated with EBG models as compared to stacked patch with no EBG model. The gain at 28GHz of all EBG models are close to model with noEBG.

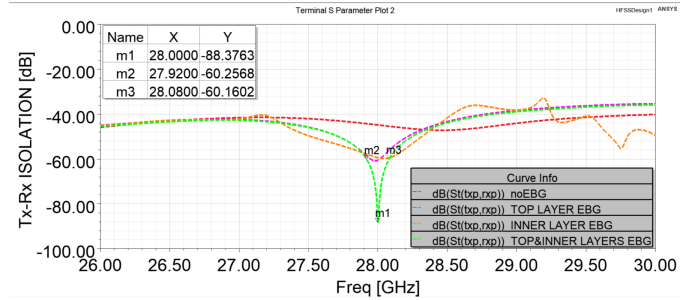


Fig. 11. Tx-Rx isolation plots of stacked patch antennas (three with integrated EBG and one with no EBG). The Top&Inner layer integrated EBG provides more than 80 dB of isolation at 28 GHz frequency. All three models with integrated EBG show at least 60 dB of isolation across 160 MHz bandwidth. These EBG integrated models provide a minimum of 16 dB of additional isolation compared to the no EBG stacked patch antenna model.

V. CONCLUSION

We studied the impact of EBG placement in a stacked patch antenna model to reduce SI and enable FD wireless. Specifically, we focused on mmWave bands, considered a mushroom EBG structure, and a 4-layer substrate stacked patch antenna design. We considered three different EBG placement models and optimized each design through a combination of theoretical models and simulations. We next conducted extensive HFSS simulations and showed that EBG integration at both top and inner substrate layers provides the highest SI isolation of more than 80 dB. We also showed that EBG integration has minimal impact on other antenna design performance metrics such as frequency bandwidth and gain.

ACKNOWLEDGEMENTS

This research was supported in part by an NSF award (CNS-1942305).

REFERENCES

- [1] A. Sabharwal, P. Schniter, D. Guo, D. W. Bliss, S. Rangarajan, and R. Wichman, "In-band full-duplex wireless: challenges and opportunities," in *IEEE Journal on Selected Areas in Communications*, 2014.
- [2] N. Reiskarimian, M. B. Dastjerdi, J. Zhou, and H. Krishnaswamy, "Analysis and design of commutation-based circulator-receivers for integrated full-duplex wireless," in *IEEE Journal of Solid State Circuits*, 2018.

- [3] A. K. Oladeinde, E. Aryafar, and B. Pejcinovic, "EBG-based self-interference cancellation to enable mmwave full-duplex wireless," in *Proceedings of IEEE Texas Symposium on Wireless and Microwave Circuits and Systems*, 2021.
- [4] C. Neo and Y. H. Lee, "Patch antenna enhancement using a mushroom-like EBG structures," in *IEEE Antenna and Propagation Society international Symposium*, 2013.
- [5] "3D electromagnetic field simulator for RF and wireless design," <https://www.ansys.com/products/electronics/ansys-hfss>.
- [6] "Ro3000 series circuit material: Ro3003, ro3006, ro3010 and ro3035 high frequency laminate," Available at: <https://www.rogerscorp.com>.
- [7] F. Yang and Y. Rahmat-Samii, *Electromagnetic band gap structures in antenna engineering*, Cambridge University Press, New York, NY, USA, 2008.
- [8] S. Dey, S. Dey, and S. K. Koul, "Isolation improvement of MIMO Antenna using novel EBG and hair-Pin Shaped DGS at 5G millimeter wave band," in *IEEE Access*, 2021.
- [9] Y. Yang and Y. Rahmat-Samii, "Microstrip antennas integrated with electromagnetic band-gap (EBG) structures: A low mutual coupling design for array applications," in *IEEE Transactions on Antennas and Propagation*, 2003.
- [10] G. Gnanagurunathan and U. Udofia, "Performance analysis of the mushroom-like-EBG structure integrated with a microstrip patch antenna," in *Proceedings of IEEE Asia-Pacific Conference on Applied Electromagnetics (APACE)*, 2010.
- [11] D. Mirshekar-Syahkal P.Deo and G. Zheng, "EBG Enhanced Broadband Dual Antenna Configuration for Passive Self-Interference Suppression in Full-Duplex Communications," in *Proceedings of the 48th European Microwave Conference*, 2018.